JOURNAL OF THERMOPHYSICS AND HEAT TRANSFER
Vol. 21, No. 1, January–March 2007

Using Input Estimation to Estimate Heat Source in Nonlinear Heat Conduction Problem

Tsung-Chien Chen* and Chung-Hsin Cheng†
National Defense University, Taoyuan 335, Taiwan, Republic of China
and
Horng-Yuan Jang‡ and Pan-Chio Tuan§
Nan Kai Institute of Technology, Nantou 542, Taiwan, Republic of China

DOI: 10.2514/1.22371

The nonlinear heat conduction problem will become more complicated when the thermal conductivity is a quadratic temperature function and the volumetric heat capacity is a linear temperature function. In this paper, the input estimation algorithm, including the extended Kalman filter and the weighted recursive least-squares estimator , is proposed to estimate the unknown time-varying heat source in this nonlinear heat conduction problem. The simulation results show that the proposed algorithm can estimate the unknown time-varying heat source online with more accuracy. If the nonlinear heat conduction problem is regarded as the linear heat conduction problem, the differences of the temperature distribution and the unknown time-varying heat source estimated by the Kalman filter with the weighted recursive least-squares estimator are also illustrated in this work.

Nomenclature

B	=	sensitivity matrix
C	=	volumetric heat capacity
c_p	=	specific heat
c_0	=	coefficient
c_1	=	coefficient
F_T	=	Jacobian matrix
F_φ	=	Jacobian matrix
H	=	measurement matrix
K	=	Kalman gain
K_b	=	gain of input estimation
k_0	=	coefficient
k_1	=	coefficient
k_2	=	coefficient
L	=	slab thickness
M	=	sensitivity matrix
N	=	total number of spatial nodes
P	=	error covariance matrix
Q_d	=	process noise covariance
R	=	measurement error covariance
s	=	innovation covariance
T	=	temperature
t	=	time
γ	=	weighted factor
Δt	=	sampling time
δ	=	Dirac delta function
θ	=	dimensionless temperature
κ	=	thermal conductivity
ν	=	measurement error
ρ	=	density
Φ	=	state transition matrix
φ	=	heat source

Superscripts

T	=	transpose of matrix
-	=	dimensionless variable
*	=	nominal denote
^	=	estimated

I. Introduction

THE heat conduction problem becomes nonlinear if the thermal properties are temperature-dependent. Nonlinearity is much less an issue in the case that the temperature gradient is small in the nonlinear heat conduction problem. When there exits a large temperature difference, nonlinearity sometimes will become very important. The main source of the thermal nonlinearity is that the thermal conductivity and the volumetric heat capacity ρc_p are dependent on temperature. It is necessary for the engineering applications to understand the effects of nonlinearity in the heat conduction problem. What is the relationship between the thermal conductivity and the volumetric heat capacity with varying temperature? From previous researchers, there are several findings as follows. Chen [1] assumed that the thermal conductivity is a linear temperature function and the volumetric heat capacity ρc_p is a constant. Huang [2] assumed that κ and ρc_p vary linearly with temperature. Gutierrez [3] assumed that κ is a linear temperature function and ρc_p is a quadratic temperature function. Besides, Marta and Vladimir [4] assumed that κ and ρc_p are both the temperature exponential functions. This research assumes that the thermal conductivity is a quadratic function of temperature, and the volumetric heat capacity is a linear temperature function. Furthermore, it is to use the inverse estimation method to estimate the unknown time-varying heat source in the nonlinear heat conduction problem (NHCP). There are various theories about the inverse heat conduction problem (IHCP), and the development of the solutions has already been in progress constantly. Those solutions can be assorted into two major categories in terms of the data processing. One is the offline estimation [2,5–8] and the other is the online estimation [9–12]. The offline estimation processes the data in the batch form. The problem with the batch form is the computational inefficiency. To resolve the inefficiency issue of the batch form approach, Tuan et al. [9] in 1996 successfully developed an input

Received 10 January 2006; revision received 25 May 2006; accepted for publication 6 July 2006. Copyright © 2006 by the American Institute of Aeronautics and Astronautics, Inc. All rights reserved. Copies of this paper may be made for personal or internal use, on condition that the copier pay the $10.00 per-copy fee to the Copyright Clearance Center, Inc., 222 Rosewood Drive, Danvers, MA 01923; include the code $10.00 in correspondence with the CCC.

*Associate Professor, Department of System Engineering, Chung Cheng Institute of Technology; chojan@ccit.edu.tw.

†Graduate Student, Department of System Engineering, Chung Cheng Institute of Technology; g960402@ccit.edu.tw.

‡Assistant Professor, Department of Computer Science and Information Engineering; jghgyn@nkc.edu.tw.

§Professor, Department of Computer Science & Information Engineering; tuan@nkc.edu.tw.

estimation algorithm, which can online estimate an unknown input, such as the heat flux, heat sources, etc., as shown in the papers presented by Tuan [9,10] and Ji [11,12]. In this research, the online estimation is applied to estimate inversely the unknown time-varying heat source in the nonlinear heat conduction problem. The reason is that many heat-transferring processes in practice are nonlinear rather than linear and many temperature related data, such as the heat flux, heat sources, and the heat conductivity, are required to be determined online for practical engineering applications. After the nonlinear heat conduction problem is built by assuming the thermal conductivity as a quadratic temperature function and the volumetric heat capacity as a linear temperature function, the state equation can be obtained by applying the finite difference algorithm to the nonlinear heat conduction problem. As a result, the input estimation algorithm, including the extended Kalman filter (EKF) and the weighted recursive least-squares estimator (WRLSE), is proposed to estimate the unknown time-varying heat source online in the nonlinear heat conduction problem.

II. Problem Formulation

Assume that a thermal slab with the thickness L and an unknown heat source $\varphi(t)$ is applied at the position $x = x_b$. Both boundaries are insulated at $x = 0$ and $x = L$. The thermal conductivity is $\kappa(T)$, and $\rho c_p(T)$ is the volumetric heat capacity that will change with the variation in temperature. The assumptions are made as follows:

$$\kappa(T) = k_0 + k_1(T - T_0) + k_2(T - T_0)^2 \tag{1}$$

$$C(T) = \rho c_p(T) = c_0 + c_1(T - T_0) \tag{2}$$

In the preceding equations, T_0 is the initial temperature of the slab at $t = 0$. The mathematical formulation of the one-dimensional transient nonlinear heat conduction problem can be defined as follows:

$$C(T)\frac{\partial T}{\partial t} = \frac{\partial}{\partial x}\left(\kappa(T)\frac{\partial T}{\partial x}\right) + \varphi(t)\delta(x - x_b), \quad 0 < x < L, \quad 0 < t \leq t_f \tag{3a}$$

$$-\kappa(T)\frac{\partial T}{\partial x} = 0, \qquad x = 0 \tag{3b}$$

$$-\kappa(T)\frac{\partial T}{\partial x} = 0, \qquad x = L \tag{3c}$$

$$T(x, 0) = T_0 \tag{3d}$$

where $T(x, t)$ is the temperature distribution as a function of x and t, and x is the position of the slab. The unknown heat source is $\varphi(t)$ applied at the position $x = x_b$, and the Direc delta function represents

$$\delta(x - x_b) = \begin{cases} 1 & x = x_b \\ 0 & \text{others} \end{cases}$$

The measured temperature $z_m(t)$ is obtained from the thermocouple at the position $x = L$. The measurement equation is defined as follows:

$$z_m(t) = HT(x, t) + \nu(t), \qquad x = L \tag{4}$$

where $H = [0, \ldots, 1]$ is the measurement matrix and $\nu(t)$ is the measurement error, which is assumed to be the Gaussian white noise with zero mean. Figure 1 illustrates the geometry and coordinates of this nonlinear heat conduction problem.

To verify the assumption that the thermal conductivity can be the quadratic temperature function, that is,

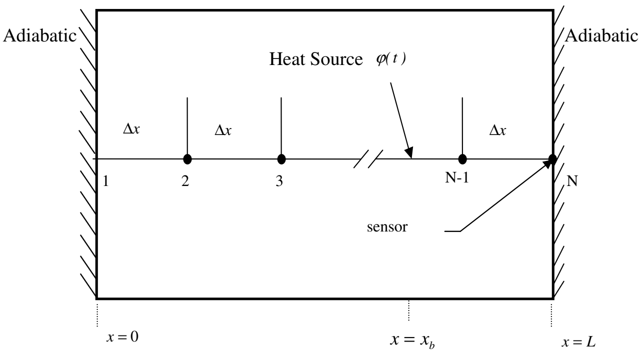

Fig. 1 Geometry and Coordinates of 1-D NHCP.

$$\kappa(T) = k_0 + k_1(T - T_0) + k_2(T - T_0)^2$$

we take the element Fe as an example. The properties of Fe are shown in Table 1. Using the regression analysis to analyze the data in Table 1, the thermal conductivity of Fe can be obtained as a second-order polynomial of the temperature and the coefficients, which are as follows:

$$k_0 = 75.89\ \text{W/m°C}, \qquad k_1 = -0.0854\ \text{W/m(°C)}^2$$
$$k_2 = 0.00004386\ \text{W/m(°C)}^3$$

The fitting curve and the properties of Fe are shown in Fig. 2, which illustrates that it is reasonable to assume that the thermal conductivity is the quadratic temperature function. By referring to [13], the volumetric heat capacity of Fe is a linear temperature function, and the coefficients are as follows:

$$c_0 = 3450000\ \text{KJ/(m}^3\text{°C)}, \qquad c_1 = 3325\ \text{KJ/m}^3\text{(°C)}^2$$

It is convenient to make Eqs. (3a–3d) of the nonlinear heat conduction problem to be in the dimensionless forms. The dimensionless parameters are introduced as follows:

$$X = x/L, \qquad \alpha_0 = k_0/c_0, \qquad \tau = \alpha_0 t/L^2$$
$$\theta = (T - T_0)/(T_\infty - T_0) \tag{5}$$

$$\bar{C} = C/c_0 = 1 + \frac{c_1(T - T_0) + c_2(T - T_0)^2}{c_0} = 1 + \bar{c}_1\theta + \bar{c}_2\theta$$
$$\bar{c}_1 = \frac{c_1(T_\infty - T_0)}{0}, \qquad \bar{c}_2 = \frac{c_2(T_\infty - T_0)^2}{c_0} \tag{6}$$

$$\bar{\kappa} = \frac{\kappa}{k_0} = 1 + \frac{k_1(T - T_0)}{k_0} + \frac{k_2(T - T_0)^2}{k_0} = 1 + \bar{k}_1\theta + \bar{k}_2\theta^2$$
$$\bar{k}_1 = \frac{k_1(T_\infty - T_0)}{k_0}, \qquad \bar{k}_2 = \frac{k_2(T_\infty - T_0)^2}{k_0} \tag{7}$$

Table 1 The properties of Fe

Temperature (°C)	Thermal conductivity coefficient (W/m°C)
−100	87
0	73
100	67
200	62
300	55
400	48
600	40
800	36
1000	35
1200	36

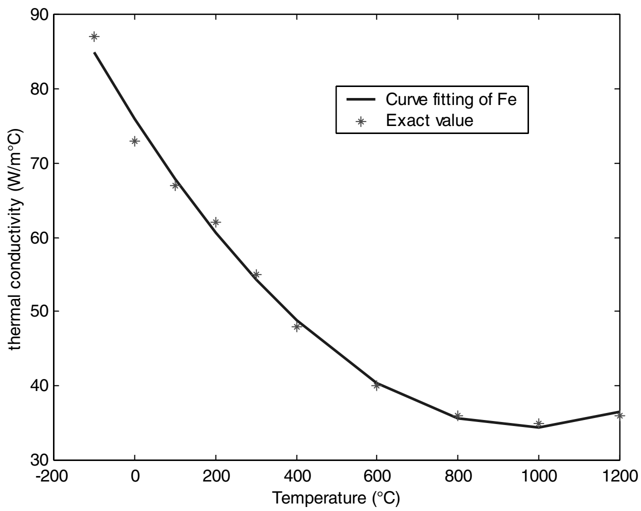

Fig. 2 Comparison between the fitting curve and the properties of Fe.

and, in addition,

$$\frac{\partial T}{\partial t} = \frac{\partial T}{\partial \tau}\frac{\partial \tau}{\partial t} = (T_\infty - T_0)\frac{\alpha_0}{L^2}\frac{\partial \theta}{\partial \tau} \tag{8}$$

$$\frac{\partial T}{\partial x} = \frac{\partial T}{\partial X}\frac{\partial X}{\partial x} = \frac{(T_\infty - T_0)}{L}\frac{\partial \theta}{\partial X} \tag{9}$$

By substituting Eqs. (5–9) in Eqs. (3a–3d) and (4), the dimensionless equations can be obtained as follows:

$$\bar{C}(\theta)\frac{\partial \theta}{\partial \tau} = \frac{\partial}{\partial X}\left[\bar{\kappa}(\theta)\frac{\partial \theta}{\partial X}\right] + \bar{\varphi}(\tau)\delta(X - X_b)$$
$$\bar{\varphi}(\tau) = \frac{L^2\varphi(t)}{k_0(T_\infty - T_0)} \tag{10}$$

The boundary conditions in Eqs. (3b) and (3c) can be rearranged in dimensionless form as follows:

$$\bar{\kappa}(\tau)\frac{\partial \theta(X,\tau)}{\partial X} = 0, \qquad X = 0 \tag{11}$$

$$\bar{\kappa}(\tau)\frac{\partial \theta(X,\tau)}{\partial X} = 0, \qquad X = 1 \tag{12}$$

The initial condition in Eq. (3d) can be expressed in the dimensionless form shown next:

$$\theta(X, 0) = 0 \tag{13}$$

The dimensionless measurement equation is defined as follows:

$$z(\tau) = H\theta(X,\tau) + \bar{\nu}(\tau), \qquad z(\tau) = \frac{z_m(t) - HT}{T_\infty - T_0}$$
$$\bar{\nu}(\tau) = \frac{\nu(t)}{T_\infty - T_0} \tag{14}$$

There are N nodes from $X = 0$ to $X = 1$, so that the slab can be divided into $N - 1$ equal blocks. Assume that the length of each block is $\Delta X = h$. Let θ_1 be the temperature at node 1, which is at the position, $X = 0$. θ_N is the temperature at node N, which is at the position $X = 1$. Based on the central difference method [14] and the boundary conditions of Eqs. (11) and (12), the relation between the temperature $\theta(X,\tau)$ and the heat source $\bar{\varphi}(t)$ in the mathematical expression can be derived. The formulating procedure is shown as follows:

$$\frac{\partial \theta(X,\tau)}{\partial \tau} = \frac{(\bar{k}_1 + 2\bar{k}_2\theta)}{\bar{C}(\theta)}\left(\frac{\partial \theta}{\partial X}\right)^2 + \frac{\bar{\kappa}(\theta)}{\bar{C}(\theta)}\frac{\partial^2 \theta}{\partial X^2} + \frac{\bar{\varphi}(\tau)}{\bar{C}(\theta)}\delta(X - X_b) \tag{15}$$

From the central difference approximation, we know that

$$\frac{\partial \theta_i}{\partial X} = \frac{\theta_{i+1} - \theta_{i-1}}{2h}, \qquad \frac{\partial^2 \theta}{\partial X^2} = \frac{\theta_{i+1} - 2\theta_i + \theta_{i-1}}{h^2} \tag{16}$$

By choosing $i = 1$, Eqs. (15) and (16) can be rearranged as shown next.

$$\dot{\theta}_1(\tau) = \frac{(\bar{k}_1 + 2\bar{k}_2\theta_1)}{\bar{C}(\theta_1)}\left(\frac{\theta_2 - \theta_0}{2h}\right)^2 + \frac{\bar{\kappa}(\theta_1)}{\bar{C}(\theta_1)}\left(\frac{\theta_2 - 2\theta_1 + \theta_0}{h^2}\right)$$
$$+ \frac{\bar{\varphi}(\tau)}{\bar{C}(\theta_1)}\delta(X - X_b) \tag{17}$$

From the boundary condition in Eq. (11), it is clear that $\theta_0(\tau) = \theta_2(\tau)$. Therefore

$$\dot{\theta}_1(\tau) = f_1 = \frac{\bar{\kappa}(\theta_1)}{\bar{C}(\theta_1)}\frac{2\theta_2 - 2\theta_1}{h^2} + \frac{\bar{\varphi}(\tau)}{\bar{C}(\theta_1)}\delta(X - X_b) \tag{18}$$

By applying $i = 2, 3, \ldots\ldots, N - 1$ to Eqs. (15) and (16), we can get

$$\dot{\theta}_1(\tau) = f_i = \frac{(\bar{k}_1 + 2\bar{k}_2\theta_i)}{\bar{C}(\theta_i)}\left(\frac{\theta_{i+1} - \theta_{i-1}}{2h}\right)^2$$
$$+ \frac{\bar{\kappa}(\theta_i)}{\bar{C}(\theta_i)}\left(\frac{\theta_{i+1} - 2\theta_i + \theta_{i-1}}{h^2}\right) + \frac{\bar{\varphi}(t)}{\bar{C}(\theta_i)}\delta(X - X_b) \tag{19}$$

Choosing $i = \text{N}$, the equality $\theta_{N+1} = \theta_{N-1}$ can be obtained from the boundary condition Eq. (12). Equations (15) and (16) can therefore be rearranged as the following equation:

$$\dot{\theta}_N(\tau) = f_N = \frac{\bar{\kappa}(\theta_N)}{\bar{C}(\theta_N)}\left(\frac{2\theta_{N-1} - 2\theta_N}{h^2}\right) + \frac{\bar{\varphi}(\tau)}{\bar{C}(\theta_N)}\delta(X - X_b) \tag{20}$$

By combining Eqs. (18–20) and taking the process noise input into account, the nonlinear continuous-time state equation can be derived as follows:

$$\dot{\theta}(\tau) = f[\theta(\tau), \bar{\varphi}(\tau), \tau] + G(\tau)\omega(\tau)$$
$$\theta(\tau) = \{\theta_1(\tau), \theta_2(\tau), \ldots, \theta_N(\tau)\}^T, \qquad f = [f_1, f_2, \cdots, f_N]^T \tag{21}$$

where $\omega(\tau)$ is white process noise and $\dot{\theta}(\tau)$ is short for $d\theta(\tau)/d\tau$.

Given a nominal input $\bar{\varphi}^*(\tau)$ and a nominal temperature $\theta^*(\tau)$ the following nominal system will be satisfied:

$$\dot{\theta}^*(\tau) = f[\theta^*(\tau), \bar{\varphi}^*(\tau), \tau]$$

Let

$$\delta\theta(\tau) = \theta(\tau) - \theta^*(\tau), \qquad \delta\bar{\varphi}(\tau) = \bar{\varphi}(\tau) - \bar{\varphi}^*(\tau)$$

then

$$\frac{\mathrm{d}}{\mathrm{d}\tau}\delta\theta(\tau) = \delta\dot{\theta}(\tau) = \dot{\theta}(\tau) - \dot{\theta}^*(\tau) = f[\theta(\tau), \bar{\varphi}(\tau), \tau] + G(\tau)\omega(\tau)$$
$$- f[\theta^*(\tau), \bar{\varphi}^*(\tau), \tau] \tag{22}$$

Expanding $f[\theta(\tau), \bar{\varphi}(\tau), \tau]$ in a Taylor series with respect to $\theta^*(\tau)$ and $\bar{\varphi}^*(\tau)$, and neglecting the higher-order terms, the following perturbation equation can be obtained:

$$\delta\dot{\theta}(\tau) = F_\theta[\theta^*(\tau), \bar{\varphi}^*(\tau), \tau]\delta\theta(\tau) + F_{\bar{\varphi}}[\theta^*(\tau), \bar{\varphi}^*(\tau), \tau]\delta\bar{\varphi}$$
$$+ G(\tau)\omega(\tau) \tag{23}$$

where F_θ and $F_{\bar\varphi}$ are $N \times N$ and $N \times 1$ Jacobian matrices, respectively. Those matrices are shown as follows:

$$F_\theta[\theta^*(\tau), \bar\varphi^*(\tau), \tau] = \begin{bmatrix} \frac{\partial f_1}{\partial \theta_1^*} & \cdots & \frac{\partial f_1}{\partial \theta_N^*} \\ \vdots & \ddots & \vdots \\ \frac{\partial f_N}{\partial \theta_1^*} & \cdots & \frac{\partial f_N}{\partial \theta_N^*} \end{bmatrix}$$

$$F_{\bar\varphi}[\theta^*(\tau), \bar\varphi^*(\tau), \tau] = \begin{bmatrix} \frac{\partial f_1}{\partial \bar\varphi^*} \\ \vdots \\ \frac{\partial f_N}{\partial \bar\varphi^*} \end{bmatrix}$$

where

$$\frac{\partial f_i}{\partial \theta_j^*} \quad \text{and} \quad \frac{\partial f_i}{\partial \bar\varphi^*}$$

are applied to be short for the following expressions:

$$\frac{\partial f_i}{\partial \theta_j^*} = \frac{\partial f_i[\theta(\tau), \bar\varphi(\tau), \tau]}{\partial \theta_j(\tau)}\bigg|_{\theta(\tau)=\theta^*(\tau), \bar\varphi(\tau)=\bar\varphi^*(\tau)}$$

$$\frac{\partial f_i}{\partial \bar\varphi^*} = \frac{\partial f_i[\theta(\tau), \bar\varphi(\tau), \tau]}{\partial \bar\varphi(\tau)}\bigg|_{\theta(\tau)=\theta^*(\tau), \bar\varphi(\tau)=\bar\varphi^*(\tau)}$$

By sampling Eq. (23) with $\Delta\tau$, the following discrete-time equation is obtained:

$$\delta\theta(k+1) = \Phi(k+1, k;^*)\delta\theta(k) + \Psi(k+1, k;^*)\delta\bar\varphi(k) + \omega_d(k) \tag{24}$$

with the terms

$$\Phi(k+1, k;^*) \cong I + F_\theta[\theta^*(k), \bar\varphi^*(k), k]\Delta\tau$$

$$\Psi(k+1, k;^*) \cong F_{\bar\varphi}[\theta^*(k), \bar\varphi^*(k), k]\Delta\tau$$

$$F_\theta[\theta^*(k), \bar\varphi^*(k), k] = \begin{bmatrix} A_{1,1} & A_{1,2} & 0 & \cdots & \cdots & \cdots & \cdots & 0 \\ A_{2,1} & A_{2,2} & A_{2,3} & \cdots & 0 & \cdots & 0 & 0 \\ 0 & A_{3,2} & A_{3,3} & A_{3,4} & 0 & \cdots & 0 & 0 \\ \vdots & & \ddots & \ddots & & & & \vdots \\ 0 & & \ddots & A_{i,i-1} & A_{i,i} & A_{i,i+1} & \ddots & 0 \\ \vdots & & & \ddots & \ddots & \ddots & & 0 \\ 0 & \cdots & \cdots & \cdots & 0 & A_{N-1,N-2} & A_{N-1,N-1} & A_{N-1,N} \\ 0 & \cdots & \cdots & \cdots & \cdots & 0 & A_{N,N-1} & A_{N,N} \end{bmatrix}$$

$$A_{1,1} = \frac{\partial f_1}{\partial \theta_1} = \frac{2}{h^2}\left[\frac{\bar C(\theta_1)(\bar k_1 + 2\bar k_2\theta_1) - \bar c_1\bar\kappa(\theta_1)}{\bar C(\theta_1)^2}(\theta_2 - \theta_1) - \frac{\bar\kappa(\theta_1)}{\bar C(\theta_1)}\right] - \frac{\bar c_1\bar\varphi(k)\delta(X - X_b)}{\bar C(\theta_1)^2}$$

$$A_{1,2} = \frac{\partial f_1}{\partial \theta_2} = \frac{2}{h^2}\frac{\bar\kappa(\theta_1)}{\bar C(\theta_1)}$$

$$A_{i,i-1} = \frac{\partial f_i}{\partial \theta_{i-1}} = \frac{1}{h^2}\frac{\bar\kappa(\theta_i)}{\bar C(\theta_i)} + \frac{1}{2h^2}\frac{\bar k_1 + 2\bar k_2\theta_i}{\bar C(\theta_i)}(\theta_{i-1} - \theta_{i+1}) \qquad i = 2\ldots N-1$$

$$A_{i,i} = \frac{\partial f_i}{\partial \theta_i} = \frac{1}{h^2}\left[\frac{\bar C(\theta_i)(\bar k_1 + 2\bar k_2\theta_i) - \bar\kappa(\theta_i)\bar c_1}{\bar C(\theta_i)^2}(\theta_{i+1} - 2\theta_i + \theta_{i-1}) - 2\frac{\bar\kappa(\theta_i)}{\bar C(\theta_i)}\right]\cdots + \frac{1}{4h^2}\left[\frac{\bar C(\theta_i)2\bar k_2 - (\bar k_1 + 2\bar k_2\theta_i)\bar c_1}{\bar C(\theta_i)^2}(\theta_{i+1} - \theta_{i-1})^2\right] - \frac{\bar c_1\bar\varphi(k)\delta(X - X_b)}{\bar C(\theta_i)^2}, \qquad i = 2\cdots N$$

$$A_{i,i+1} = \frac{\partial f_i}{\partial \theta_{i+1}} = \frac{1}{h^2}\frac{\bar\kappa(\theta_i)}{\bar C(\theta_i)} + \frac{1}{2h^2}\frac{\bar k_1 + 2\bar k_2\theta_i}{\bar C(\theta_i)}(\theta_{i+1} - \theta_{i-1}) \qquad i = 2\ldots N-1$$

$$A_{N,N-1} = \frac{\partial f_N}{\partial \theta_{N-1}} = \frac{2}{h^2}\frac{\bar\kappa(\theta_N)}{\bar C(\theta_N)}$$

$$A_{N,N} = \frac{\partial f_N}{\partial \theta_N} = \frac{2}{h^2}\left[\frac{\bar C(\theta_N)(\bar k_1 + 2\bar k_2\theta_N) - \bar c_1\bar\kappa(\theta_N)}{\bar C(\theta_N)^2}(\theta_{N-1} - \theta_N) - \frac{\bar\kappa(\theta_N)}{\bar C(\theta_N)}\right] - \frac{\bar c_1\bar\varphi(k)\delta(X - X_b)}{\bar C(\theta_N)^2}$$

$$F_{\bar\varphi}[\theta^*(k), \bar\varphi^*(k), k] = \begin{bmatrix} 0 \\ 0 \\ \vdots \\ 1 \\ \vdots \\ 0 \\ 0 \end{bmatrix} \times \frac{1}{\bar C(\theta_j)}$$

$$\omega_d(k) = \int_{k\Delta\tau}^{(k+1)\Delta\tau} \Phi(k+1, k;^*)G(k)\omega(k)d\tau$$

where $\delta\theta(k)$ represents the state vector, $\Phi(k+1, k;^*)$ is the state transition matrix, $\bar\varphi(k)$ is the heat source, and $\omega_d(k)$ is a discrete-time Gaussian sequence, which is assumed to be the white noise with zero mean and the variance

$$\mathbf{E}\{\omega_d(k)\omega_d^T(j)\} = Q_d\delta_{kj}$$

where δ_{kj} is the Dirac delta function. The discrete-time measurement equation is shown next:

$$z(k) = H\theta(k) + \bar v(k) \tag{25}$$

Where $z(k)$ represents the measurement vector at the kth time step, $H = [0, \ldots, 1]$ is the measurement matrix, and $\bar v(k)$ is the Gaussian white noise with zero mean and the variance

$$\mathbf{E}\{v(k)v^T(j)\} = \mathbf{R}\delta_{kj}$$

The input estimation algorithm, including the EKF and the WRLSE, is used in this research to estimate the unknown heat source.

III. Input Estimation Algorithm

The input estimation algorithm, including the extended Kalman filter and the weighted recursive least-squares estimator, will be used to inversely estimate the unknown time-varying heat source in the nonlinear heat conduction problem. The purpose of the extended Kalman filter is to generate the recursive innovation sequence. This sequence contains bias or systematic errors caused by implicit unknown time-variant inputs and it also contains the variance or random errors caused by the measurement errors. To resolve this situation, the weighted recursive least-squares estimator can be used to identify the sudden system error induced by the unknown time-variant input.

After the linear perturbation Eq. (23) is established, the extended Kalman filter equation can be derived. Please refer to [1] for the detailed derivation procedure. The equations are defined as follows:

$$\hat{\theta}(k+1/k) = \hat{\theta}(k/k) + \int_{k\Delta\tau}^{(k+1)\Delta\tau} f[\hat{\theta}(k/k), \bar{\varphi}^*(k), \tau]\,\mathrm{d}\tau \tag{26}$$

$$\hat{\theta}(k+1/k+1) = \hat{\theta}(k+1/k) + K(k+1;^*)[z(k+1) - H(k+1)\hat{\theta}(k+1/k)] \tag{27}$$

$$K(k+1;^*) = P(k+1/k;^*)H^T(k+1;^*)[H(k+1;^*)P(k+1;^*), H^T(k+1;^*) + R(k+1)]^{-1} \tag{28}$$

$$P(k+1/k;^*) = \Phi(k+1/k;^*)P(k+1/k;^*)\Phi^{\mathrm{T}}(k+1/k;^*) + Q_d(k+1/k;^*) \tag{29}$$

$$P(k+1/k+1;^*) = [I - K(k+1;^*)H(k+1;^*)]P(k+1;^*) \tag{30}$$

The EKF prediction equation is shown as Eq. (26), where

$$\int_{k\Delta\tau}^{(k+1)\Delta\tau} f[\hat{\theta}(k/k), \bar{\varphi}^*(k), \tau]\,\mathrm{d}\tau$$

is evaluated by means of numerical integration formulas that are initialized by

$$f[\hat{\theta}(k/k), \bar{\varphi}^*(k), k]$$

Equation (27) is the EKF correction equation. In Eqs. (28–30), * denotes the use of $\theta^*(k+1) = \hat{\theta}(k+1/k)$.

The weighed recursive least-squares estimator was presented by Tuan et al [9]. The mathematical equations are described briefly, next.

$$B(k+1) = H[\Phi M(k) + I]\Psi \tag{31}$$

$$M(k+1) = [I - K(k+1)H][\Phi M(k) + I] \tag{32}$$

$$K_b(k+1) = \gamma^{-1}P_b(k)B^T(k+1)[B(k+1)\gamma^{-1}P_b(k)B^T(k+1) + s(k+1)]^{-1} \tag{33}$$

$$P_b(k+1) = [I - K_b(k+1)B(k+1)]\gamma^{-1}P_b(k) \tag{34}$$

$$\hat{\bar{\varphi}}(k+1) = \hat{\bar{\varphi}}(k) + K_b(k+1)[\bar{z}(k+1) - B(k+1)\hat{\bar{\varphi}}(k)] \tag{35}$$

where $K(k+1)$ is the Kalman gain, $s(k+1)$ is the covariance of the residual, $\bar{z}(k+1) = z(k) - H\hat{\theta}(k+1/k)$ are obtained from the extended Kalman filter and represent the variance of the estimated input vector, $B(k+1)$ and $M(k+1)$ are the sensitivity matrices, and $\hat{\varphi}(k+1)$ is the estimated unknown input heat source. The weighted factor is usually assumed to be a constant between 0 and 1.

IV. Results and Discussion

Assume that the temperature of the environment is $T_\infty = 25°\mathrm{C}$, and the initial temperature of the slab is $T_0 = 0°\mathrm{C}$. The related coefficients with respect to the dimensionless thermal conductivity and the volumetric heat capacity of Fe can be obtained from Eqs. (6) and (7). These coefficients are as follows: $\bar{k}_1 = -0.0281$, $\bar{k}_2 = 0.000361$, and $\bar{c}_1 = 0.024$. They are used as the thermal conductivities, $\bar{\kappa}(\theta) = 1 - 0.0281\theta + 0.000361\theta^2$ and the volumetric heat capacity, $\bar{C}(\theta) = 1 + 0.024\theta$ for the nonlinear heat conduction problem, which is simulated in this paper. If the distance between any two samples of the slab ΔX is set to be 0.1, there will be 11 nodes from the position $X = 0$ to $X = 1$. The boundary conditions at both ends are assumed to be adiabatic, and three different kinds of heat sources ($\bar{\varphi}_1$, $\bar{\varphi}_2$, and $\bar{\varphi}_3$) are applied at node 6, respectively, as shown in Eqs. (36–38).

$$\bar{\varphi}_1(\tau) = \begin{cases} 10, & 0 \le \tau < 4 \\ 4 + 0.75\tau, & 4 \le \tau < 8 \\ 20 - 1.25\tau, & 8 \le \tau < 14 \\ 2.5, & 14 \le \tau \le 18 \end{cases} \tag{36}$$

$$\bar{\varphi}_2(\tau) = \begin{cases} 0, & 0 \le \tau < 5 \\ 10, & 5 \le \tau \le 10 \\ 0, & 10 \le \tau \le 18 \end{cases} \tag{37}$$

$$\bar{\varphi}_3(\tau) = \begin{cases} 0, & 0 \le \tau < 5 \\ 25, & 5 \le \tau \le 10 \\ 0, & 10 \le \tau \le 18 \end{cases} \tag{38}$$

This research is using the Runge–Kutta method to directly solve the temperature field distribution of the nonlinear heat conduction [Eq. (10)]. The temperature distributions of node 11 are illustrated in Figs. 3–5. The red solid lines in Figs. 3–5 represent the temperature distribution of node 11 when the heat sources are applied, $\bar{\varphi}_1$, $\bar{\varphi}_2$, and $\bar{\varphi}_3$, respectively. The differences will be discussed later in this section. If the nonlinear heat conduction problem is regarded as the linear heat conduction problem (i.e., while $\bar{\kappa}(\theta) = 1$ and $\bar{C}(\theta) = 1$), the temperature distributions of node 11 in the linear heat conduction problem will be solved as shown in Figs. 3–5 by using the same way with the same conditions. It can be observed that all temperature distributions of the linear heat conduction problem are higher than those of the nonlinear heat conduction problem. By comparing Fig. 4

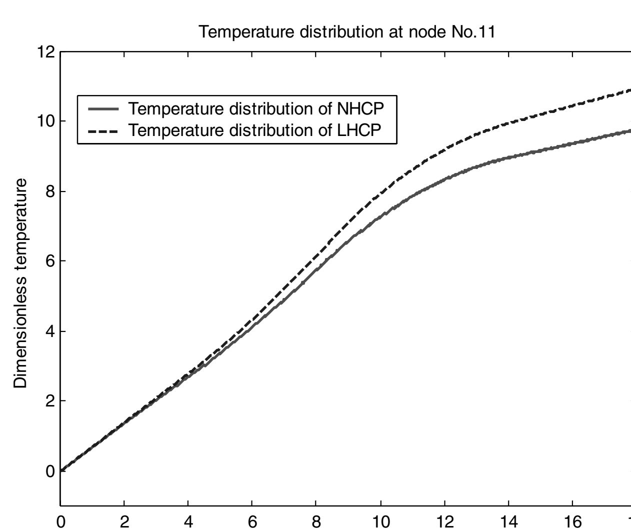

Fig. 3 Comparison between the linear and nonlinear temperature distributions when the heat source $\bar{\varphi}_1$ is applied.

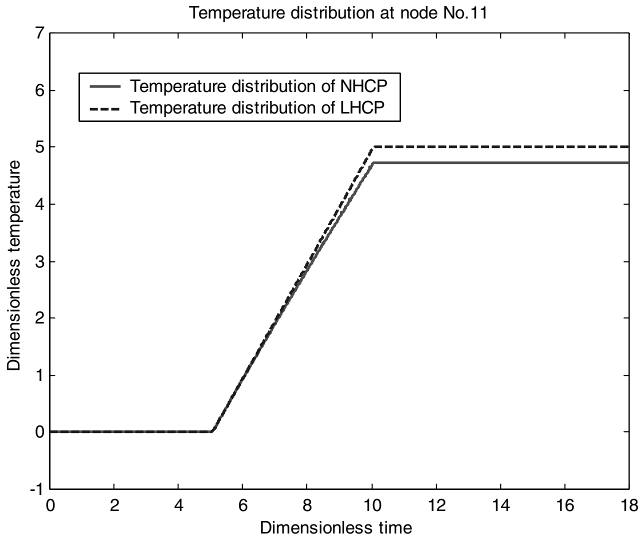

Fig. 4 Comparison between the linear and nonlinear temperature distributions when the heat source $\bar{\varphi}_2$ is applied.

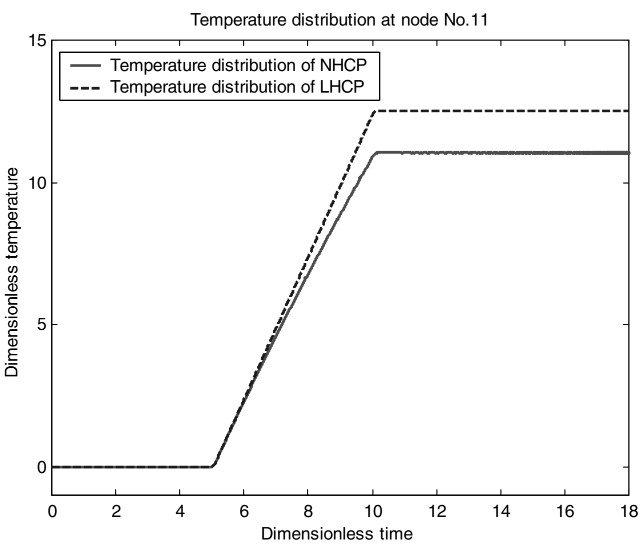

Fig. 5 Comparison between the linear and nonlinear temperature distributions when the heat source $\bar{\varphi}_3$ is applied.

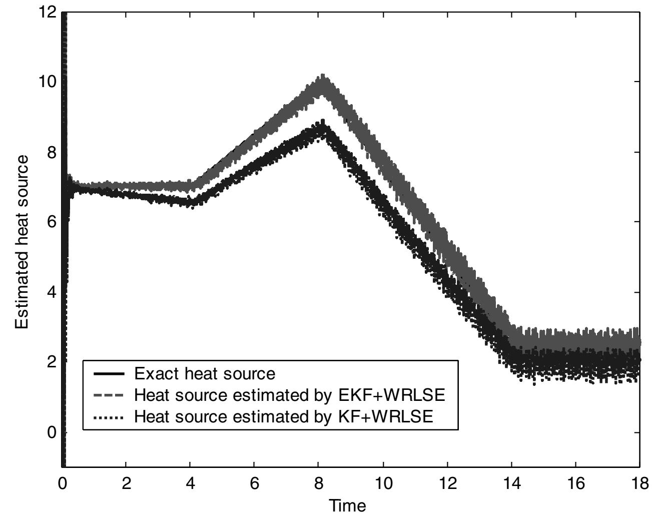

Fig. 6 Comparison between the heat source $\bar{\varphi}_1$, estimated by using the linear (KF and WRLSE) and nonlinear (EKF and WRLSE) algorithms.

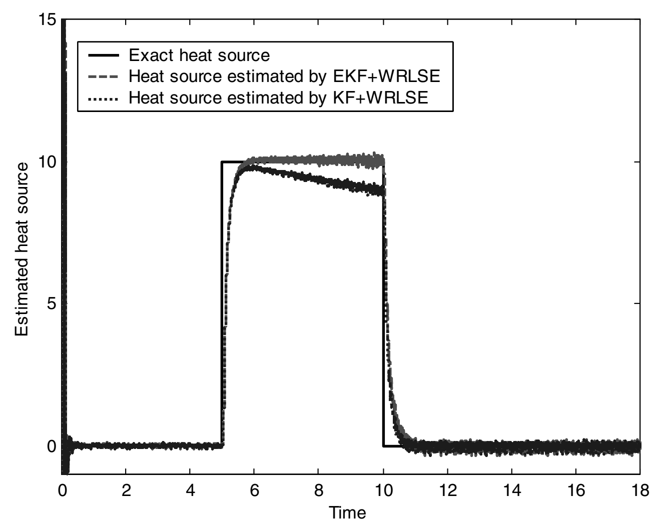

Fig. 7 Comparison between the heat source $\bar{\varphi}_2$, estimated by using the linear (KF and WRLSE) and nonlinear (EKF and WRLSE) algorithms.

with Fig. 5, it is clear to see that the temperature difference between the linear heat conduction problem and the nonlinear heat conduction problem is even greater when the heat source becomes stronger. The reason is that the volumetric heat capacity increases and the thermal conductivity decreases as the temperature rises. This results in the reduction of the variation in temperature, $\partial\theta/\partial\tau$ in Eq. (10), so that more energy will be required to raise the temperature of the nonlinear heat conduction problem. Besides, the temperature distribution in the nonlinear heat conduction problem will be lower than that in the linear heat conduction problem, and the difference between the two will be greater as the heat source intensifies.

To verify the accuracy of using the input estimation algorithm, including the EKF and the WRLSE, to estimate the unknown heat source in the nonlinear heat conduction problem, three examples are used to explain the availability of this method. Assume that the sampling time is $\Delta\tau = 0.001$. The initial conditions of the EKF are as follows: $\hat{\theta}(0/0) = [0 \quad 0 \quad \cdots \quad 0]^T$, $Q_d = 10^{-8}$, and $P(0/0) =$ diag$[10^2]$. The initial conditions of the WRLSE are as follows: $\hat{\varphi}(0) = 0$, $P_b(0) = 10^2$, and $M(0) = 0$. The weighted factor is set to be 0.95. A thermocouple is assumed to be located at node 11 to measure the temperature, which is actually computed by using the simulation method. That is to say, the measurement temperature $z(t)$ can be obtained by directly solving the temperature distribution (the red solid lines in Figs. 3–5) at node 11 in the nonlinear heat conduction problem and adding a random measurement error $\bar{v}(\tau)$. The covariance of the random measurement error is set to be $R = 10^{-6}$. Based on the measurement temperature, the unknown heat sources $\bar{\varphi}_1$, $\bar{\varphi}_2$, and $\bar{\varphi}_3$ can be estimated by using the EKF and WRLSE algorithms separately. The red lines in Figs. 6–8 are showing the results. As mentioned before, if the nonlinear heat conduction problem is regarded as the linear heat conduction problem, the algorithm including the KF and the WRLSE [9] is used to estimate the unknown heat sources $\bar{\varphi}_1$, $\bar{\varphi}_2$, and $\bar{\varphi}_3$ separately. The blue lines in Figs. 6–8 show the results, respectively. From the comparison of Figs. 6–8, it shows that the algorithm, including the EKF and the WRLSE, can estimate the unknown heat sources online accurately. However, the results derived from KF and WRLSE generates greater errors. Besides, the errors will enlarge if the heat source becomes stronger. The reason is that more heat is required to raise the temperature in the nonlinear heat conduction problem than the linear one. When using the same measurement temperature to inversely estimate the unknown heat source in the linear conduction problem, it is clear that the estimated heat source value in the linear heat conduction problem will be lower than the actual value of heat source. In spite of this situation, the combined algorithm of the EKF and the WRLSE has good performance in tracking the time-varying unknown heat source in the NHCP. Therefore, if there are materials whose thermal conductivity and volumetric heat capacity are

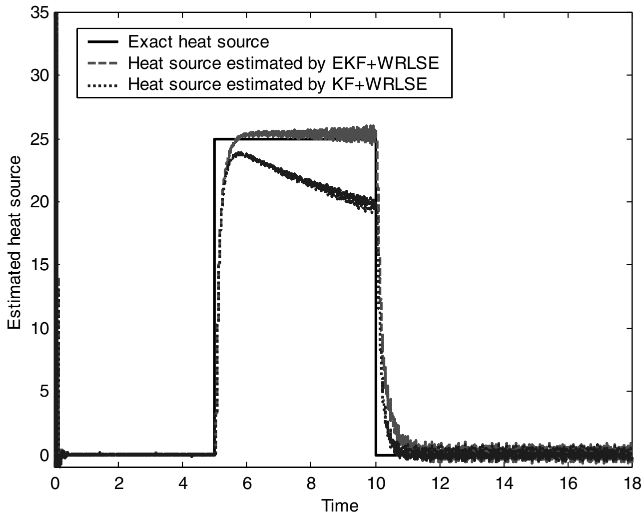

Fig. 8 Comparison between the heat source $\bar{\varphi}_3$ estimated by using the linear (KF and WRLSE) and nonlinear (EKF and WRLSE) algorithms.

temperature-dependent, the heat source estimation error will be larger by using the linear approach. On the other hand, the nonlinear approach, which is based on the combined algorithm of the EKF and the WRLSE, will be obtaining a good performance of the unknown heat source estimation.

V. Conclusion

When the temperature function of the thermal conductivity is quadratic and the temperature function of the volumetric heat capacity is linear, it is a complicated nonlinear heat conduction problem and the nonlinearity will be enhanced as the temperature gradient becomes greater. In this case, the temperature distribution and unknown time-varying heat source estimation will cause greater errors than the actual values if the NHCP is regarded as the LHCP presented in this paper. The simulated results also prove that the input estimation algorithm, including the EKF and the WRLSE, can accurately estimate the unknown time-varying heat source in the nonlinear heat conduction problem in real time. Therefore, the algorithm proposed in this research is proven to be effective in solving the nonlinear heat conduction problem.

References

[1] Wang, H. M., Chen, T. C., Tuan, P. C., and Den, S. G., "Adaptive-Weighting Input-Estimation Approach to Nonlinear Inverse Heat-Conduction Problems," *Journal of Thermophysics and Heat Transfer*, Vol. 19, No. 2, Apr.–June 2005, pp. 211–212.

[2] Huang, C. H., and Ozisik, M. N., "Inverse Problem of Determining Unknown Wall Heat Flux in Laminar Flow Through a Parallel Plat Duct," *Numerical Heat Transfer, Part A, Applications*, Vol. 21, No. 1, 1992, pp. 55–70.

[3] Gutierrez, G., and Jen, T. C., "Numerical Simulation of Nonlinear Heat Conduction Subjected to a Laser Source: The Effects of Variable Thermal Properties," *International Journal of Heat and Mass Transfer*, Vol. 43, No. 12, 2000, pp. 2177–2192.

[4] Marta, R., and Vladimir, S., "Studies on the Nonlinearity Effects in Dynamic Compact Model Generation of Packages," *IEEE Transactions on Components and Packaging Technologies*, Vol. 27, No. 1, Mar. 2004, pp. 124–130.

[5] Alifanov, O. M., and Millhailov, V. V., "Solution of the Nonlinear Inverse Thermal Conducting Problem by the Iteration Method," *Journal of Engineering Physics*, Vol. 35, No. 6, 1978, pp. 1501–1506.

[6] Mikhailov, V. V., "Questions of the Convergence of Iteration Methods of Solving the Inverse Heat Conduction Problem," *Journal of Engineering Physics*, Vol. 48, No. 5, 1984, pp. 1263–1265.

[7] Scott, E. P., and Beck, J. V., "Analysis of Order of the Sequential Regularization Solutions of Inverse Heat Conduction Problem," *Journal of Heat Transfer*, Vol. 111, No. 2, 1989, pp. 218–224.

[8] Huang, C. H., and Wang, Y. C., "Inverse Problem of Controlling the Interface Velocity in Stefan Problems by Conjugate Gradient Method," *Journal of the Chinese Institute of Engineers*, Vol. 19, No. 2, 1996, pp. 247–253.

[9] Tuan, P. C., Fong, L. W., and Huang, W. T., "Analysis of On-line Inverse Heat Conduction Problems," *Journal of Chung Cheng Institute of Technology*, Vol. 25, No. 1, 1996, pp. 59–73.

[10] Tuan, P. C., Fong, L. W., and Huang, W. T., "Application of Kalman Filtering with Input Estimation Technique to On-line Cylindrical Inverse Heat Conduction Problems," *JSME International Journal, Series B (Fluids and Thermal Engineering)*, Vol. 40, No. 1, 1997, pp. 126–133.

[11] Ji, C. C., Tuan, P. C., and Jang, H. Y., "A Recursive Least-Squares Algorithm for On-line 1-D Inverse Heat Conduction Estimation," *International Journal of Heat and Mass Transfer*, Vol. 40, No. 9, 1997, pp. 2081–2096.

[12] Ji, C. C., and Jang, H. Y., "An Inverse Problem in Predicting Heat Flux of M42 Percussion Primer," *Journal of the Franklin Institute*, Vol. 335B, No. 4, 1998, pp. 595–604.

[13] Touloukian, Y. S., *Thermophysical Properties of Matter*, TPRC Data Series, IFI/PLENUM, New York, 1970.

[14] D'Souza, N., "Numerical Solution of One-Dimensional Inverse Transient Heat Conduction by Finite Difference Method," ASME Paper 75-WA/HT-81, 1975.